

Vacuum Stability as a Guide for Model Building

Gudrun Hiller,^{a,b} Tim Höhne,^a Daniel F. Litim,^b and Tom Steudtner^{a,c}

^a*Department of Physics, TU Dortmund, Otto-Hahn-Str.4, D-44221 Dortmund, Germany*

^b*Department of Physics and Astronomy, University of Sussex, Brighton, BN1 9QH, U.K.*

^c*Department of Physics, University of Cincinnati, Cincinnati, OH 45221, USA*

We explain why vector-like fermions are natural candidates to lift the Standard Model vacuum instability. Results are further discussed from the viewpoint of criticality. Several models allow for vector-like quarks and leptons in the TeV-range which can be searched for at the LHC.

1 Introduction

The discovery of the Higgs particle together with theoretical precision calculations evidenced the instability of the standard model (SM) vacuum.^{1,2,3} While a theory of nature with a decaying ground state would be unacceptable, vacuum metastability due to a lifetime sufficiently large compared to the age of the universe has become a widely accepted narrative. Further, the continuing success of the SM in the LHC era, with only a few anomalies and the absence of clear new physics signatures at colliders or elsewhere, calls for new ideas and directions in model building. In this contribution, we promote the quest for vacuum stability into a primary model building task.⁴ The rationale for this is that while the onset of the SM instability is a high energy effect, unattainable by present or planned future colliders, its existence alone does not point towards a specific scale for new physics. Therefore, solutions could emerge from novel phenomena at any scale below the Planck scale, and potentially as low as a few TeV.

2 Vacuum Stability

We begin by taking stock of vacuum stability in the SM. To that end, we study the 3-loop running of SM couplings up to the Planck scale and beyond.^{4,5,6} We introduce the $U(1)_Y \times SU(2)_L \times SU(3)_c$ gauge couplings g_ℓ ($\ell = 1, 2, 3$), the top and bottom Yukawa interactions $y_{t,b}$, and the Higgs quartic λ , all normalized in units of loop factors, and write them as

$$\alpha_\ell = \frac{g_\ell^2}{(4\pi)^2}, \quad \alpha_{t,b} = \frac{y_{t,b}^2}{(4\pi)^2}, \quad \alpha_\lambda = \frac{\lambda}{(4\pi)^2}. \quad (1)$$

SM initial conditions (central values) are determined at the reference scale $\mu_0 = 1$ TeV. The uncertainties in the initial values due to the strong gauge coupling, Higgs and W mass are quantitatively irrelevant. The dominant source of uncertainty originates from the determination of the top mass $m_t = 172.76 \pm 0.30$ GeV,⁷ which is indicated in Fig. 1 by a 1σ uncertainty band for all couplings. Due to its smallness, the bottom Yukawa $\alpha_b(\mu)$ is not displayed even though it is retained in the numerics.

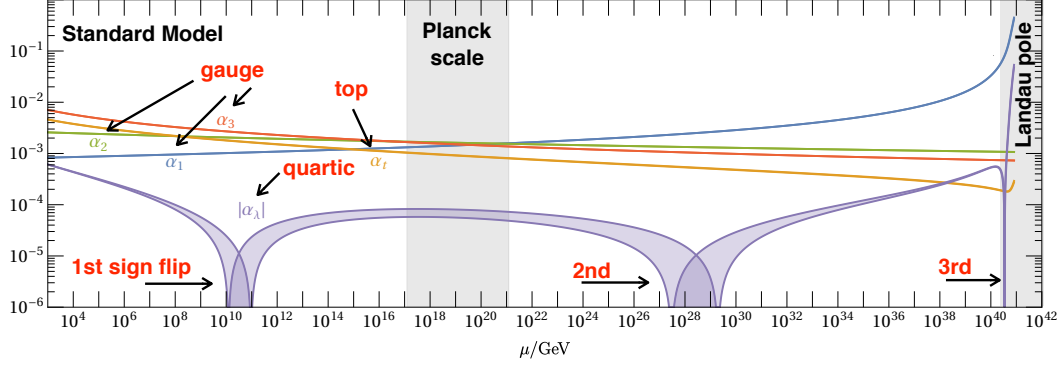


Figure 1 – Shown is the Standard Model 3-loop running of the Higgs quartic, top Yukawa, and gauge couplings above TeV energies. The vacuum becomes unstable ($\mu \approx 10^{10}$ GeV) prior to the Planck scale (center gray band). Subsequently, and ignoring quantum gravity effects, the steady growth of the hypercharge coupling re-instates stability ($\mu \approx 10^{29}$ GeV) much before perturbativity, stability, and predictivity are ultimately lost at a Landau pole ($\mu \approx 10^{41}$ GeV). Bands indicate a 1σ uncertainty in the top pole mass.

Unsurprisingly, Fig. 1 confirms that SM couplings run slowly. Most notably, however, and within uncertainties, the Higgs quartic invariably displays a sign flip around $\mu \approx 10^{10}$ GeV, signaled by a downward spike, and indicating the onset of vacuum instability. Stability up to the Planck scale would require that the top mass deviates by more than 3σ from its presently determined central value. Hence, a negative value for the Higgs quartic at the Planck scale

$$\alpha_\lambda|_{\mu=M_{\text{Pl}}} \approx -10^{-4} \quad (2)$$

and the possibility of an unstable “great desert” should be taken for real. Curiously, extending the flow beyond the Planck scale, we observe that the Higgs becomes stable again ($\mu_{\text{stab}} \approx 10^{10} M_{\text{Pl}}$), largely triggered by the mild but continued growth of the hypercharge coupling. At much higher energies ($\mu_{\text{Landau}} \approx 10^{13} \mu_{\text{stab}}$), however, stability, perturbativity, and predictivity are ultimately lost, in this order and for good, and the SM as we know it comes to an end. Hence, new effects are required to stabilise the vacuum, either straight out of quantum gravity, or from particle physics via new matter fields or interactions.

3 Model Building Directions

Vacuum stability can be achieved through BSM effects, as long as these enhance the Higgs quartic sufficiently strongly.⁴ Minimally, this can be done by introducing new particles which only couple to the SM gauge fields (“gauge portals”). One may also introduce new interactions involving the Higgs and the BSM fields such as new Yukawas (“Yukawa portal”) or new quartics (“Higgs portal”), or other; see^{6,8,9} for recent examples. Gauge portals only modify parameters of the SM beta functions and lead to mild effects. Yukawa, Higgs, and other portals add new interactions, and thereby modify the running of couplings more significantly.^{4,6,8,9}

The main idea for the gauge portal mechanism⁴ could not be any simpler: add N_F new vector-like fermions (VLF) to the SM, with charges (Y_F, d_2, d_3) under the $U(1)_Y \times SU(2)_L \times SU(3)_c$ gauge group. By design, any of these SM extensions are free of gauge anomalies, and allow for Dirac mass terms M_F ,

$$\mathcal{L}_{\text{BSM}} \supset \bar{\psi} (i\not{D} - M_F) \psi. \quad (3)$$

From the viewpoint of the renormalisation group (RG), the primary effect is that the new particles modify the running of gauge couplings. Specifically, gauge beta functions $\beta_i \approx -B_i \alpha_i^2$ have modified one-loop coefficients $B_1 = -\frac{41}{3} - \delta B_1$, $B_2 = \frac{19}{3} - \delta B_2$, and $B_3 = 14 - \delta B_3$, with positive VLF contributions $\delta B_1 = \frac{8}{3} N_F d_2 d_3 Y_F^2$ and $\delta B_{2,3} = \frac{8}{3} N_F d_{3,2} S_2(d_{2,3})$ in terms of their hypercharge Y_F and Dynkin indices $S_2(d_{2,3})$ under $SU(2)_L$ and $SU(3)_c$.

Let us briefly explain how new matter fields modify the running of the Higgs quartic. For simplicity, we take the BSM fermion mass as the matching scale $\mu_0 = M_F$ to SM running. VLFs then decouple at scales below their own mass, and contribute as if they were massless at scales above. Subleading threshold corrections are neglected. For RG scales $\Lambda > \mu_0$, $\delta B_i \geq 0$ implies that gauge couplings take values larger or equal to their SM values,

$$\alpha_\ell(\Lambda) - \alpha_\ell^{\text{SM}}(\Lambda) \geq 0. \quad (4)$$

For the top Yukawa, we observe from $\beta_t \approx \alpha_t [9\alpha_t - \frac{17}{6}\alpha_1 - \frac{9}{2}\alpha_2 - 16\alpha_3]$ that all gauge couplings contribute negatively to its leading order running. Together with (4), we conclude that the top Yukawa becomes smaller than in the SM,

$$\alpha_t(\Lambda) - \alpha_t^{\text{SM}}(\Lambda) < 0. \quad (5)$$

Finally, we turn to the Higgs quartic coupling α_λ . Given that its value is much smaller than the top Yukawa and gauge couplings, Fig. 1, its running is primarily driven by the inhomogeneous terms, $\beta_\lambda \approx \frac{3}{8} [\alpha_1^2 + 2\alpha_1\alpha_2 + 3\alpha_2^2] - 6\alpha_t^2$. Most notably, the gauge and top Yukawa couplings contribute with opposite signs, which in view of (4) and (5) means that they all pull into the same direction. Overall, the Higgs quartic is invariably enhanced over its SM value,

$$\alpha_\lambda(\Lambda) - \alpha_\lambda^{\text{SM}}(\Lambda) > 0. \quad (6)$$

This is the gauge portal mechanism. We conclude that vector-like fermions are natural candidates to stabilise the electroweak vacuum. It then remains to be seen whether the uplift (6) is sufficient to offset metastability (2). To leading logarithmic accuracy, we find

$$\begin{aligned} \alpha_\lambda(\Lambda) - \alpha_\lambda^{\text{SM}}(\Lambda) \approx & \frac{3}{8}\alpha_1^2(\mu_0) [\alpha_1(\mu_0) + \alpha_2(\mu_0)] \delta B_1 \ln^2(\Lambda/\mu_0) \\ & + \frac{3}{8}\alpha_2^2(\mu_0) [\alpha_1(\mu_0) + 3\alpha_2(\mu_0)] \delta B_2 \ln^2(\Lambda/\mu_0) \\ & + 32\alpha_t^2(\mu_0) \alpha_3^2(\mu_0) \delta B_3 \ln^3(\Lambda/\mu_0) + \text{subleading}. \end{aligned} \quad (7)$$

A few comments are in order. (i) The leading impact from the hypercharge and weak isospin interactions, characterized by the terms $\propto \delta B_{1,2} \ln^2(\Lambda/\mu_0)$, originates from the direct uplift of the Higgs quartic at 2-loop level and leading logarithmic accuracy. (ii) Since the Higgs is colourless, the leading impact from strong interactions is channeled through the top Yukawa coupling, and $\propto \delta B_3 \ln^3(\Lambda/\mu_0)$ instead. The additional loop suppression may very well be compensated by the sizeable prefactor, also depending on VLF masses, gauge charges and multiplicities. (iii) Since the leading loop coefficients of the scalar and top Yukawa beta functions have not changed, the modified running of gauge couplings implies that α_λ approximately runs along the SM trajectory $\alpha_\lambda(\mu) \approx \alpha_\lambda^{\text{SM}}(\mu_{\text{SM}})$, though with an altered “RG velocity”. From (4) we have $\mu_{\text{SM}}(\mu) \gtrsim \mu$ for the weak and strong portals, effectively uplifting α_λ . For the hypercharge portal we find that $\mu_{\text{SM}}(\mu) < \mu$ instead, and the α_λ trajectory comes out as a “squeezed” version of the SM one. The general case is a combination of these two effects. (iv) In any gauge portal extension, the Higgs quartic is naturally bounded from below by its most negative value achieved along the SM trajectory, and, incidentally, given by its value at the Planck scale, (2).

4 Gauge Portals at Work

To illustrate how the gauge portal mechanism (6) operates quantitatively, we numerically integrate the full 2-loop RG running,^{4,5} starting with the weak gauge portal characterized by N_F new vector-like leptons (VLLs) of mass M_F in the representation $(0, d_2, 1)$. A concrete example ($N_F = 5, M_F = 1$ TeV) is shown in Fig. 2 (left panel). The new VLLs induce a small uplift of the weak gauge coupling (solid, green), just enough to stabilise the Higgs quartic (solid violet) along the trajectory up to the Planck scale. In Fig. 2 (right panel), we perform a parameter

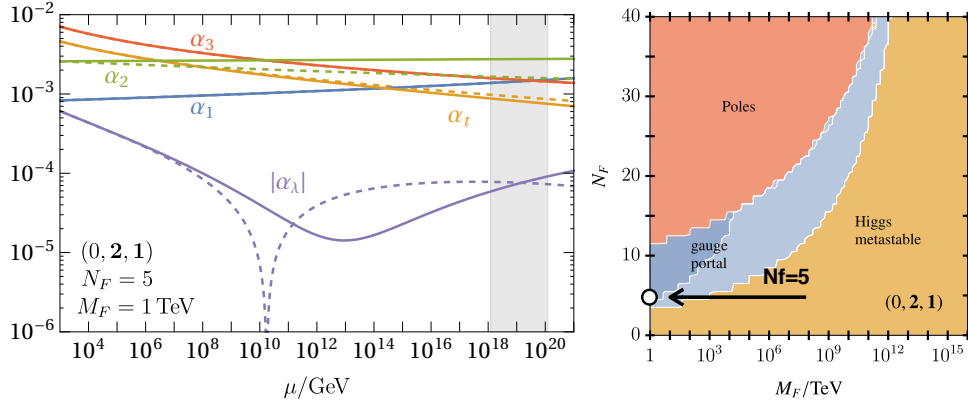


Figure 2 – Illustration of the weak gauge portal for SM extensions with N_F generations of VLLs of mass M_F and in the representation $(0, \mathbf{2}, \mathbf{1})$. Left panel: VLLs generate sufficient uplift in comparison with SM running (full vs dashed lines). Right panel: critical surface of parameters in the (N_F, M_F) plane, indicating whether the Planck scale vacuum is metastable (yellow), stable at or all the way up to the Planck scale (light vs dark blue), or plagued by a subplanckian Landau pole in α_2 (red). The left panel model parameters are also indicated (white dot). The weak gauge portal extends substantially into the high mass and high multiplicity region.

scan in the (N_F, M_F) plane to identify the “critical surface”, i.e. the BSM parameter regions where the potential at the Planck scale is stable (blue), metastable (yellow), or plagued by a subplanckian Landau pole (red). If M_F is too large and N_F too small, there is not enough RG time to lift the instability, and the effects are “too little too late”. On the other hand, if N_F is too large and M_F too small, the effects are too strong and predictivity is lost due to a Landau pole prior to the Planck scale. The sweet spot of SM extensions with stable vacua is situated in the wedge between the regions of metastability and Landau poles, which covers a wide range of multiplicities N_F and masses M_F . We also find regions where the uplift (6) ensures stability all the way up to M_{Pl} (dark blue), and regions where “squeezing” dominates (light blue). We notice that there is no upper limit on N_F nor M_F . Larger M_F implies that gauge couplings are much smaller at the matching scale. However, as long as subplanckian Landau poles are avoided, the smallness can be countered by larger N_F , which allows α_2 to grow fast enough to stabilise the Higgs.

Interestingly, very similar results are found for the strong gauge portal,^{4,10} even though α_3 contributions are loop-suppressed over α_2 contributions (7). Considering N_F VLFs of mass M_F in the representation $(0, \mathbf{1}, d_3 < \mathbf{10})$ we again find wedges of stability, much like in Fig. 2. Unlike in the weak gauge portal, however, we now observe upper bounds on N_F and on M_F , for example $M_F \lesssim 10^6 \text{ TeV}$ and $2 \leq N_F \leq 18$ for vector-like quarks ($d_3 = \mathbf{3}$).⁴ The reason for this is that for too large M_F , α_3 and α_t at the matching scale are too small to generate sufficient uplift (6). In fact, even if asymptotic freedom is lost (for large N_F), the growth of α_3 and the induced decrease of α_t are insufficient to generate stability.

Finally, we consider the hypercharge portal characterized by N_F VLLs of mass M_F in the representation $(Y_F, \mathbf{1}, \mathbf{1})$. Most interestingly, also the hypercharge portal is available, despite the looming Landau pole. The critical surface of parameters is shown exemplarily for models with $Y_F = \frac{1}{2}$ in Fig. 3 (right panel). Once more, we observe a stability wedge between regions of metastability and Landau poles. Unlike the weak and strong portals, however, we do not find any region where $\alpha_\lambda > 0$ all the way up to the Planck scale, showing that the uplift in (7) from hypercharge alone is insufficient. Instead, stability arises through “squeezing”, as illustrated in Fig. 3 (left panel) for $N_F = 32$ and several values for M_F (correspondingly highlighted by dots in the right panel). Given that α_1 is larger than α_1^{SM} , we recognise the new α_λ trajectories in Fig. 3 as increasingly squeezed versions of the SM trajectory in Fig. 1. Evidently, the effect is more pronounced for smaller M_F as this triggers an earlier start of the accelerated α_1 growth. If squeezing is too substantial, even the third sign change may arise prior to the Planck scale, typically around $\alpha_1 \gtrsim \text{few} \times 10^{-2}$, followed by an imminent Landau pole.

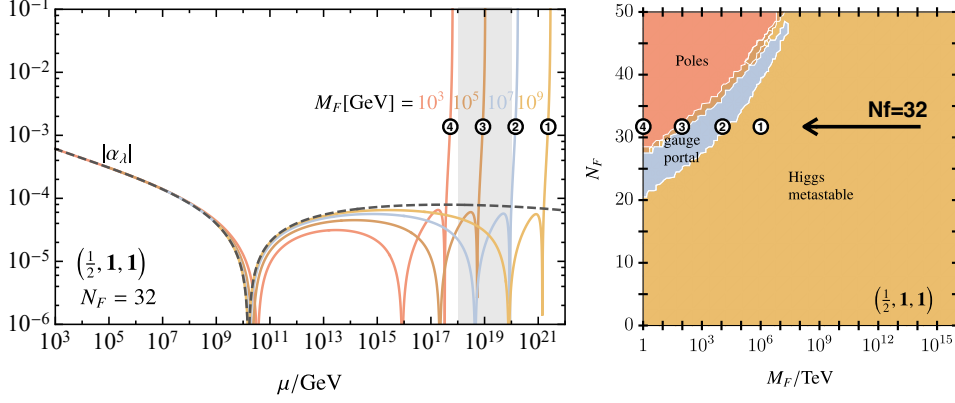


Figure 3 – Illustration of the hypercharge portal for SM extensions with N_F generations of VLLs of mass M_F and in the representation $(\frac{1}{2}, \mathbf{1}, \mathbf{1})$, showing the critical surface of parameters in the (N_F, M_F) plane (right panel), colour-coding as in Fig. 2. The left panel highlights the running of the BSM Higgs quartic in comparison to SM running (dashed line) for $N_F = 32$ and four different M_F , with corresponding dots also shown in the right panel. We observe that the “squeezing” effect delivers Planck-scale stability whereas the uplift is insufficient.

The hypercharge portal disappears either by increasing M_F thus leaving insufficient RG time for squeezing to be operative, or by increasing N_F leading to a subplanckian theory breakdown. Increasing the hypercharge $|Y_F|$ causes the N_F -window to become narrower and to move towards lower N_F , and vice versa for $Y_F \leftrightarrow N_F$. Maximal hypercharges are achieved for smallest number of flavours, and increasing M_F for fixed N_F enhances the overall range of viable Y_F .

5 How Critical is the Standard Model?

It has been noticed previously¹¹ that the SM Higgs quartic is near-critical, with $\beta_\lambda|_{\mu=M_{\text{Pl}}} \approx 0$ and $\alpha_\lambda|_{\mu=M_{\text{Pl}}} \approx -10^{-4}$, reminiscent of a free RG fixed point at the Planck scale. It is natural to ask whether SM extensions can be found where the quartic and its beta function vanish identically. We can answer this question to the affirmative: the gauge portal mechanism allows us to find many suitable parameters (N_F, M_F) and gauge charges (Y, d_2, d_3) for VLFs such that α_λ achieves strict criticality, meaning a double-zero at a scale $M_F \leq \mu_{\text{crit}} \leq M_{\text{Pl}}$,

$$\alpha_\lambda|_{\mu_{\text{crit}}} = 0 \quad \text{and} \quad \beta_\lambda|_{\mu_{\text{crit}}} = 0. \quad (8)$$

This is illustrated in Fig. 4 where the BSM Higgs quartic α_λ remains positive throughout and achieves a double-zero just above $\mu_{\text{crit}} \approx 10^{15}$ GeV before settling around $\alpha_\lambda \approx +10^{-5}$ at the Planck scale. As a result, many SM extensions can be found where the Higgs is as or more critical than in the SM, with the added benefit of stability rather than meta-stability.

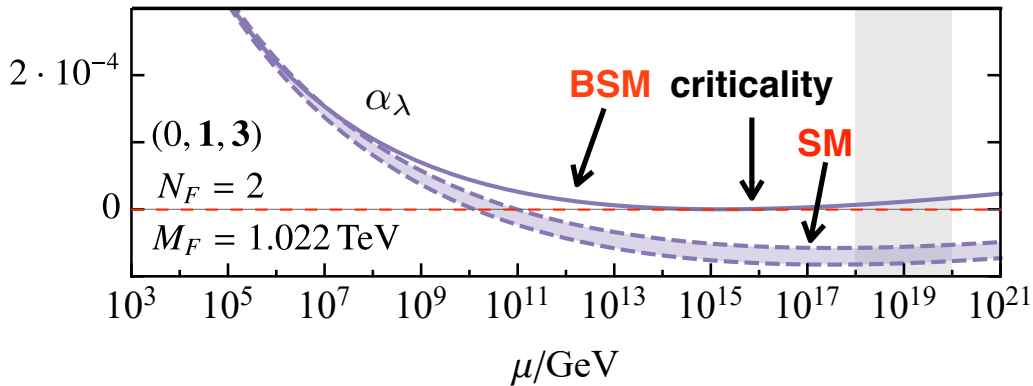


Figure 4 – Comparison of BSM and SM Higgs criticality, exemplarily for a SM extension with two vector-like quarks with charges $(0, \mathbf{1}, \mathbf{3})$ and mass $M_F = 1.022$ TeV ($m_t = 172.76$ GeV).

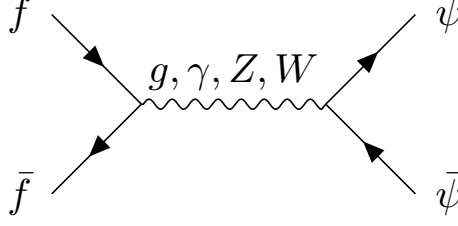


Figure 5 – Pair-production of vector-like fermions ψ at pp and $\ell\ell$ colliders, with f indicating SM quarks or leptons.

6 Discussion

Lifting the instability of the SM vacuum has been put forward as a genuine “bottom-up” model building task. SM extensions by VLFs are particularly efficient for this because the gauge portal mechanism enhances the Higgs quartic naturally, (6). Therefore, SM extensions with suitably charged VLLs and VLQs over a large range of masses are well-motivated. Moreover, searches at colliders and beyond, with broad signatures and production channels such as those indicated in Fig. 5, are strongly encouraged. Further avenues towards stability arise in extensions with additional Yukawa or Higgs portals, giving BSM parameter constraints analogous to those shown in Fig. 2 and Fig. 3.^{4,6,8,9} Settings with feeble or no Yukawas to the Higgs can be searched for in R -hadron-signatures, or di-jets.¹² Models which allow for flavourful Yukawas give rise to flavourful constraints⁴, and allow to additionally address flavour anomalies.^{6,8,9}

Acknowledgments

DFL acknowledges support by the Science Technology and Facilities Council (STFC) through the Consolidated Grant ST/T00102X/1.

References

1. S. Chatrchyan *et al.* [CMS], Phys. Lett. B **716** (2012), 30-61 [1207.7235 [hep-ex]].
2. G. Aad *et al.* [ATLAS], Phys. Lett. B **716** (2012) 1 [1207.7214 [hep-ex]].
3. G. Degrandi, S. Di Vita, J. Elias-Miro, J. R. Espinosa, G. F. Giudice, G. Isidori and A. Strumia, JHEP **08** (2012) 098 [1205.6497 [hep-ph]].
4. G. Hiller, T. Höhne, D. F. Litim and T. Steudtner, Phys. Rev. D **106** (2022) 115004 [2207.07737 [hep-ph]].
5. D. F. Litim and T. Steudtner, Comput. Phys. Commun. **265** (2021) 108021 [2012.12955 [hep-ph]].
6. G. Hiller, C. Hormigos-Feliu, D. F. Litim and T. Steudtner, Phys. Rev. D **102** (2020) 071901 [1910.14062 [hep-ph]]. Phys. Rev. D **102** (2020) 095023 [2008.08606 [hep-ph]].
7. P. A. Zyla *et al.* [Particle Data Group], PTEP **2020** (2020) 083C01
8. S. Bißmann, G. Hiller, C. Hormigos-Feliu and D. F. Litim, Eur. Phys. J. C **81** (2021) 101 [2011.12964 [hep-ph]].
9. R. Bause, G. Hiller, T. Höhne, D. F. Litim and T. Steudtner, Eur. Phys. J. C **82** (2022) 42 [2109.06201 [hep-ph]].
10. S. Gopalakrishna and A. Velusamy, Phys. Rev. D **99** (2019) 115020 [1812.11303 [hep-ph]].
11. D. Buttazzo, G. Degrandi, P. P. Giardino, G. F. Giudice, F. Sala, A. Salvio and A. Strumia, JHEP **12** (2013), 089 [1307.3536 [hep-ph]].
12. A. D. Bond, G. Hiller, K. Kowalska and D. F. Litim, JHEP **08** (2017) 004 [1702.01727 [hep-ph]], K. Kowalska, A. D. Bond, G. Hiller and D. F. Litim, PoS **EPS-HEP2017** (2017) 542.